GEOPHYSICS, VOL. 70, NO. 5 (SEPTEMBER-OCTOBER 2005); P. L45–L51, 4 FIGS., 2 TABLES.
10.1190/1.2073883

3D multiple-source Werner deconvolution for magnetic data

R. O. Hansen[1]

ABSTRACT

Werner deconvolution has been widely used for at least 30 years for rapid interpretation of magnetic data. Since 1993, a multiple-source generalization of the method has been known, and at least two implementations of the algorithm are in use. Recently, Werner deconvolution has been extended to three dimensions through the use of generalized Hilbert transforms. In this paper, a multiple-source extension of the 3D Werner algorithm is developed which also generalizes the 2D multiple-source algorithm. The implementation of this algorithm is tested on both 3D multiple-source synthetic data, for which good agreement with the model is obtained, and on complex data from the Albuquerque basin, which yields results corresponding well with other interpretations and with known geology.

INTRODUCTION

Werner deconvolution has been a workhorse of magnetic interpretation for at least 30 years (Hartman et al., 1971). However, its use has been eclipsed somewhat in recent years by Euler deconvolution because the latter method extends easily to three dimensions (Reid et al., 1990). Furthermore, Euler deconvolution can be extended in three dimensions to a multiple-source algorithm (Hansen and Suciu, 2002).

The 3D Euler algorithm, while powerful, has some limitations. The multiple-source Euler method requires taking high-order derivatives of the field, one derivative order for each source, which makes the algorithm highly dependent on data quality. The multiple-source Werner method only requires first-order derivatives, no matter the number of sources. An additional advantage of the 2D Werner method is that it produces dip angle and susceptibility contrast information in addition to depths and locations. It seems likely that a 3D Werner method would have a similar advantage, an issue discussed later in this paper.

Conversely, existing Werner deconvolution algorithms are more limited than Euler deconvolution in the source types that can be solved for (Li, 2003). In this paper, I confine the development to the traditional source types for Werner deconvolution. Although Werner deconvolution can be extended to the same range of source types as Euler deconvolution, this observation is beyond the scope of the present work and will be the subject of a future paper.

Mushayandebvu et al. (2001) introduced extended Euler deconvolution in which the dip angle and susceptibility contrast information for 2D structures are recovered from a second Euler equation. Nabighian and Hansen (2001) show that extended Euler deconvolution is a generalization of Werner deconvolution and that, like Euler deconvolution, this generalization of Werner deconvolution can be extended to three dimensions. This extension can be taken as the definition of 3D Werner deconvolution. It is then natural to ask whether the (2D) multiple-source Werner algorithm of Hansen and Simmonds (1993) can be extended to three dimensions. Hansen and Simmonds (1993) conjecture that this cannot be done; it turns out that this conjecture is wrong. However, it is unlikely that the way to proceed would have become apparent without the development of the multiple-source Euler algorithm and of the 3D extended Euler scheme.

The remainder of this paper is organized as follows. In the following section, the theoretical framework is stated (details for the two-source case are relegated to Appendix A), followed by some remarks about the implementation. Synthetic and real data examples are shown to demonstrate the utility and limitations of the algorithm. Next, the status of calculating dip angles and susceptibility contrasts is reviewed. The paper concludes with a discussion and some conclusions.

DEPTH ESTIMATION

I consider 3D magnetic sources of structural index zero (Reid et al., 1990). A precise characterization of this class of sources does not appear to be known; in the multiple-source case, the class includes at least finite collections of uniform polyhedra. This class is sufficiently general to model most

Manuscript received by the Editor August 19, 2003; revised manuscript received November 17, 2004; published online September 8, 2005.
[1]Pearson, de Ridder and Johnson, Inc., 12640 W. Cedar Dr., Suite 100, Lakewood, Colorado 80228. E-mail: rohansen@prj.com.

sources with nonzero volume, although the number of vertices, and therefore the number of sources to be solved for, may be impracticably large. At the end of this section, I discuss the modifications required to handle magnetic sources of structural index one (i.e., dike-like bodies) and gravity fields.

Data are assumed to be collected on, or continued to, a level surface (Ostrowski et al., 1993). In principle this limitation could be relaxed, but the technique for doing so would be equivalent to performing a continuation; the data might just as well be continued to a datum before processing. The multiple-source Werner algorithm shares this limitation with most other depth-estimation techniques, including the Euler method, as long as single-component (e.g., total-field) anomalies are the measured input data.

The generalized Euler equations 10 and 13 of Nabighian and Hansen (2001)

$$(x-x_0)\frac{\partial M}{\partial \xi}+(y-y_0)\frac{\partial M}{\partial \eta}+(z-z_0)\frac{\partial M}{\partial \zeta}+nM=\alpha,$$

$$(x-x_0)\frac{\partial}{\partial x}\mathcal{H}(M)+(y-y_0)\frac{\partial}{\partial y}\mathcal{H}(M)+(z-z_0)\frac{\partial}{\partial z}\mathcal{H}(M)+n\mathcal{H}(M)=\beta,$$

for structural index zero can be combined into a single equation in tensor form as

$$(R_i-R_{0i})\nabla_i\mathcal{H}_jM=\alpha_j, \tag{1}$$

where R_i is the ith component of the observation location, R_{0i} is the ith component of the source location, ∇_i is the ith component of the spatial derivative, and $\mathcal{H}_j$ is given by

$$\begin{aligned}\mathcal{H}_1&=\mathcal{H}_x,\\ \mathcal{H}_2&=\mathcal{H}_y,\\ \mathcal{H}_3&=1.\end{aligned} \tag{2}$$

Here, $\mathcal{H}_x$ and $\mathcal{H}_y$ are the x- and y-components of Nabighian's (1984) generalized Hilbert transform. The function M may be any solution of Laplace's equation, which is also homogeneous with Euler index zero in the sense of Reid et al. (1990), and α_j is the jth component of a vector from which the susceptibility contrast, dip, and strike angle of a contact can be computed [see Nabighian (1972) for the 2D case; the 3D version can be obtained easily by applying a rotation].

Nabighian and Hansen (2001) show that the 2D version of equation 1 is equivalent to the Hansen and Simmonds (1993) form of the single-source Werner equation. Thus, equation 1 may be taken as the definition of the single-source Werner equation in three dimensions. The idea is to generalize equation 1 to the case of multiple sources, along the lines of Hansen and Simmond's (1993) 2D multiple-source Werner algorithm.

The technique for generalizing the single-source algorithm is mostly easily understood in the two-source case, where the calculations can be done explicitly. This case is developed in Appendix A. Here, I proceed directly to give the result for m sources.

Following precisely the induction strategy as in the appendix of Hansen and Simmonds (1993) for the profile case, the 3D multiple source Werner equation for m sources is obtained in the form

$$\begin{aligned}&\sum_{k=0}^{m-1}a_{kji_1i_2\cdots i_k}r_{i_1}r_{i_2}\cdots r_{i_k}\\ &\quad+\sum_{k=0}^{m-1}b_{ki_1i_2\cdots i_{m-k}}r_{m-k+1}r_{m-k+2}\cdots r_m\nabla_j\mathcal{H}_{i_1}\mathcal{H}_{i_2}\cdots\mathcal{H}_{i_m}M\\ &\quad+r_{i_1}r_{i_2}\cdots r_{i_m}\nabla_j\mathcal{H}_{i_1}\mathcal{H}_{i_2}\cdots\mathcal{H}_{i_m}M=0.\end{aligned} \tag{3}$$

The notation for the coefficients is chosen to match as closely as possible that of Hansen and Simmonds (1993), but the coefficients $b_{ki_1i_2\cdots i_{m-k}}$ are the same as those that occur in multiple-source Euler deconvolution. The bs are related to the coefficients $A_{ki_1i_2\cdots i_k}$ defined in equation 34 of Hansen and Suciu (2002) by

$$b_{ki_1i_2\cdots i_{m-k}}=A_{m-ki_1i_2\cdots i_{m-k}}, \tag{4}$$

i.e., by a simple reverse ordering. It follows that the entire development of the technique for extracting the source locations R_{pi} can be used intact from the multiple-source Euler algorithm.

The coefficients $a_{kji_1i_2\cdots i_k}$ define constants $\alpha_{pji_1i_2\cdots i_{m-1}}$ by

$$\begin{aligned}\prod_{\substack{q=1\\q\neq p}}^{m}(R_{pi_q}-R_{qi_q})\alpha_{pji_1i_2\cdots i_{p-1}i_{p+1}\cdots i_m}&\\ =-\sum_{k=0}^{m-1}a_{kji_1i_2\cdots i_k}R_{pi_1}R_{pi_2}\cdots R_{pi_k}.&\end{aligned} \tag{5}$$

In the 2D case, the alphas define the susceptibility contrast, dip, and strike angle of a magnetic contact. For more general source types, their interpretation is problematic, as discussed later.

Only a very minor modification to the algorithm is required to handle sources of structural index one, traditionally associated with thin sheets or dikes. Starting with the single-source extended Euler equation for a source of this type, it is straightforward to show that the multiple-source Werner algorithm in this case is obtained by substituting a Hilbert transform for the derivative in equation 3. I omit the proof, which is merely a reiteration of the steps leading to the equation for sources of index zero. Gravity sources are also easily treated by performing a (usually vertical) derivative to yield a pseudomagnetic field. The theory for magnetic fields then applies without change.

IMPLEMENTATION

The implementation of the 3D multiple-source Werner algorithm shares a great deal with multiple-source Euler deconvolution; refer to Hansen and Suciu (2002) for details. The essential idea is to solve equation 3 as a least-squares system, followed by extraction of the source locations R_{pi} from the b coefficients.

The Hilbert transforms required for the least-squares problem are calculated in the spatial frequency domain as a batch preprocessing step. These operations can be performed on the entire grid at one time. Further processing proceeds on windows extracted from the grid; the selection of windows is discussed in the "Program Usage" section.

A key feature of the present algorithm, shared with other Werner deconvolution methods and with Euler deconvolution algorithms, is that because the initial step in the solution process is the solution of a linear least-squares problem, no starting values are required. The linear least-squares solution provides data for a nonlinear problem that is a generalization of finding the roots of a complex polynomial. This nonlinear problem, which yields the locations of the sources, is comparatively tame in the sense that finding the roots of a complex polynomial is a relatively tractable problem. Thus, the main advantage of this and all related algorithms is that they divide the problem into two steps, the first of which requires fitting to the data but is linear and the second of which is nonlinear but more tractable than, say, direct inversion for the source locations.

The least-squares problem is formulated as an overdetermined system and is solved using QR decomposition (Dongarra et al., 1979). Unlike the multiple-source Euler algorithm, this system can be solved for as large a number of sources as is required; then one can extract the coefficients for a smaller number of sources by truncating the solution. In this, the new algorithm shares the efficiency of the profile multiple-source Werner algorithm. However, to achieve this one must column orthogonalize the least-squares matrix with respect to the coefficients of the *b*s. This is done using explicit orthogonalization tables calculated analytically, which limits the practical number of sources in each data window to five. This number is large enough for any reasonable data set, based on experience with the multiple-source Euler algorithm.

An issue that arises in the least-squares fit is the use of regional terms. A constant regional is easily accommodated; the analysis of Hansen and Simmonds (1993) extends to the 3D case virtually unchanged. The net result is an increase of one in the maximum order of the generalized polynomial terms (the terms involving the *a*s). This has been incorporated into the present algorithm based on its usefulness in the 2D case.

Once the *b*s have been calculated, the source locations are extracted from the generalized polynomial, which has the *b*s as coefficients using the generalized Durand-Kerner method exactly as in the multiple-source Euler algorithm. Refer to Hansen and Suciu (2002) for details, which are carried over completely unchanged to the present algorithm.

PROGRAM USE

In Hansen and Suciu (2002) a technique is presented for determining window locations and sizes which relies heavily on hand selection. Further experience shows that while this technique produces good results, it is extremely slow. Because it is so labor intensive, it yields a very small number of depth estimates in practice. Use has therefore evolved to a more traditional moving-window scheme followed by selection from the resulting large number of depth estimates.

The selection of windows is not a fundamental part of the algorithm. One alternative is to sweep a window of fixed size through the data; this strategy is commonly used in 2D Werner programs (Hartman et al., 1971). However, this strategy lacks appeal because it seems likely to generate many duplicate location estimates. The 2D multiple-source Werner program of Hansen and Simmonds (1993) uses the analytic signal to locate preferred windows, and the 3D version of this technique (Phillips, 2002) has been tested on 3D software. For maximum flexibility, the program has been written to accept a list of windows generated in any way. The only requirements are that the algorithm used give reasonable first-order estimates and that it be rapid enough not to impact the overall turnaround time significantly.

In the current methodology, depth estimates for the entire area of interest are obtained either from published data or by using some very rapid depth-estimation scheme such as the local wavenumber (SPI™) method (Thurston and Smith, 1997). A moving window is then passed through the data whose size at each location is twice the estimated depth; then the 3D multiple-source Werner depth estimates for each window are calculated. Once the main processing step is complete, the depth estimates are edited by simple selection of those results having an acceptable estimated error (usually 15% of the depth) and lying in the depth range of interest. The editing program has a clustering option which uses chi-squared analysis of the error estimates, but this has been found to be unnecessary.

This technique contrasts sharply with that of Hansen and Suciu (2002) and reflects our prediction that the program's use might evolve with experience. In this case, the evolution has been toward a more commonly used methodology.

DEPTH ESTIMATES FOR SYNTHETIC DATA

An example used extensively in testing the multiple-source Euler algorithm is the tetrahedron sketched in Figure 1. The top vertex is at a depth of 5 grid units, and the bottom vertices are at a depth of 15 grid units. The example is challenging because the top vertex dominates the anomaly and the locations of the bottom vertices are poorly resolved.

The depth estimates in this case were obtained from a single 50-grid-unit × 50-grid-unit window centered over the source, and only the four-source solution was retained. The actual and computed locations of the source points are listed in Table 1. The top vertex and the two southern bottom vertices are located with good accuracy; the northern bottom vertex is somewhat too deep. Overall, the results are not quite as accurate as those obtained with the multiple-source Euler algorithm. Presumably, this reflects the larger number of degrees of freedom in the Werner algorithm associated with the dip angle

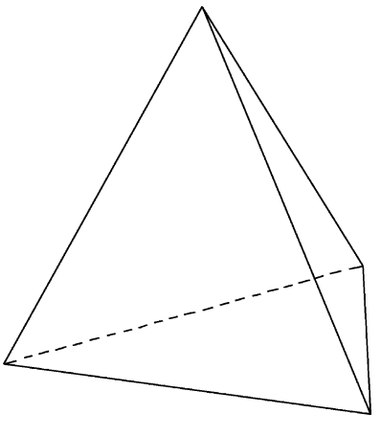

Figure 1. Sketch of the tetrahedral body used in testing.

and physical property information. Overall, however, the results are quite satisfactory.

The same data were tested with a series of small windows centered over the shallow vertex. For these windows, the three deeper vertices are effectively invisible; as expected, only the single-source solutions, listed in Table 2, were useful. These are all somewhat shallow, but the vertex is correctly located in the horizontal direction and the results give some reassurance that the program functions correctly in the single-source limit. The interpretation of this result is discussed later.

Note that the single-source depth estimates in Table 2 become systematically shallower as the size of the window increases. Presumably, this reflects the fact that as the window size increases, the influence of the deeper vertices becomes more important. For the 50×50 unit window used to obtain the accurate four-source estimates, the single-source depth estimate is -1.64. Thus, the algorithm gives some indication of grossly incorrect estimates of the number of sources.

DEPTH ESTIMATES FOR THE ISLETA-KIRTLAND SURVEY

In 1997, Sander Geophysics Ltd. acquired an aeromagnetic survey for the U.S. Geological Survey over the Isleta-Kirtland area south of Albuquerque, New Mexico (U.S. Geological Survey, 1998). The survey, flown at a line spacing of 150 m and nominal terrain clearance of 150 m, was part of a program to improve the understanding of the geologic and hydrogeologic framework of the middle Rio Grande basin.

Figure 2 shows the total magnetic intensity for the area. Although the dominant part of the signal is attributable to basement structure, there is a significant amount of magnetic source material in the near surface, as discussed by Grauch (2001). The objective of her analysis was to map shallow faults that control hydrologic flow by finding the depth offset in sedimentary marker beds containing significant quantities of magnetic material. Such an offset should appear as a two-source solution to the 3D Werner algorithm. Only depth estimates in the first 500 m below ground are relevant to this objective.

Table 1. Actual and computed locations for the tetrahedral body.

Actual x	Computed x	Actual y	Computed y	Actual z	Computed z
50.00	50.01	50.00	50.04	5.00	5.03
40.00	39.73	40.00	40.84	15.00	16.07
60.00	60.34	40.00	40.95	15.00	16.42
50.00	50.01	60.00	60.78	15.00	19.74

Table 2. Single-source depth estimates for the top vertex of the polyhedron.

Window size	Computed depth
3.0	4.04
4.0	3.98
5.0	3.90
6.0	3.82
10.0	3.38

Note that with the window selection criterion of twice the estimated depth, the minimum window size is only 300 m (ground clearance is 150 m) or two flight-line spacings. Thus, shallow anomalies are minimally sampled in the cross-track direction. However, since the dominant strike is across the flight-line direction in general, this window size should be adequate.

Local wavenumber (SPI) (Thurston and Smith, 1997) depth estimates are used as initial values for the multiple-source Werner program. These initial values are shown in Figure 3.

The multiple-source Werner program yields approximately 180 000 depth estimates in the range of 0 to 500 m, using all models ranging between one and four sources. Four-source models appear empirically to be the largest useful models on real data. The results are plotted in Figure 4. Note the excellent spatial coherence of the depth estimates, which probably correspond mainly to shallow faults. These results also agree well with interpretations performed independently on the data (Grauch, 2001; Phillips, 2002).

DIP ANGLE AND SUSCEPTIBILITY CONTRAST

Since determining the source locations follows directly from the multiple-source Euler development, the solution of equation 5 is the only remaining problem. If the source is a magnetic contact, a simple procedure reduces this to the profile

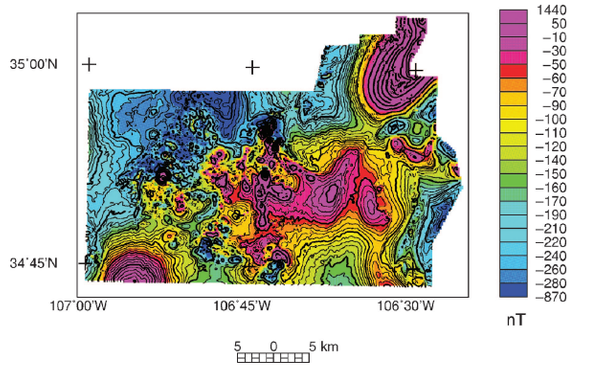

Figure 2. Total magnetic intensity for the Isleta-Kirtland area.

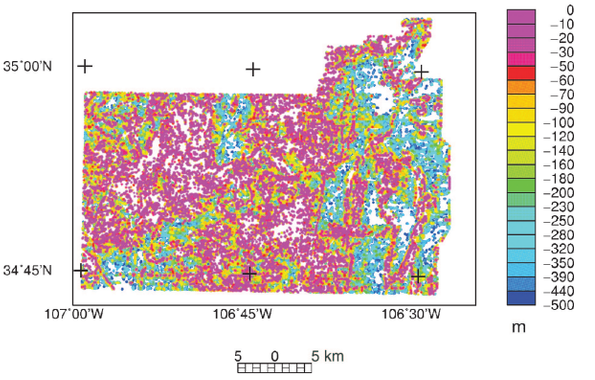

Figure 3. Local wavenumber depth estimates in meters below surface used to seed the multiple-source Werner program.

multiple-source problem. Apply a rotation in the xy-plane which eliminates the y-component of the equation. Then, since $\alpha_{pji_1i_2\cdots i_{m-1}}$ is symmetric in all its indices, the y-component of each index vanishes, i.e., it is effectively a 2D tensor. Since the tensor is also trace free, it has only two independent components — the two components of the 2D α. Thus, equation 5 reduces to two equations in two unknowns. At this stage, it is actually easier to rewrite the equation as a single complex equation — equation 9 of Hansen and Simmonds (1993) — and solve it by synthetic division. The strike angle is determined by the rotation angle required to set the y-component of equation 5 to zero.

However, tests of the dip angle and susceptibility contrast calculations produced disappointing results. To generate values that could be interpreted easily, a model consisting of a single dipping interface was constructed and used to test the program. This model yielded nonsensical results for the depths and locations (as a result, the dip angle and susceptibility were also meaningless).

Some further testing and an examination of previous model results provided an explanation that agrees with the conclusions of Mushayandebvu et al. (2004) for the extended Euler method. They found that the extended Euler equations have a zero eigenvalue when the source is two dimensional; the corresponding eigenvector points along the strike direction. When the single dipping interface is replaced by two interfaces intersecting at a corner, the program correctly locates the top and bottom of the corner. Furthermore, in the tetrahedral model previously discussed, the program locates the vertices of the tetrahedron. Thus, the depths and locations that the program finds are not arbitrary along 2D features but are the corners at which these features intersect.

The problem is then to interpret the dip angle and susceptibility quantities at the intersection of 2D structures, i.e., at a vertex. The key to doing so rests in the solution to what is, apparently, an open problem. Hansen and Wang (1988) show that the gravity and magnetic fields of a homogeneous polyhedron can be written in the frequency domain as a sum of contributions corresponding to the vertices of the polyhedron. However, H. Holstein (personal communication, 2003) points out that the magnetic field of a polyhedron, all but one of whose vertices have been moved to infinity, must be infinite because, by similarity, this is equivalent to moving the observation point to a vertex of a finite polyhedron. The magnetic field at a vertex of a polyhedron is known to be singular.

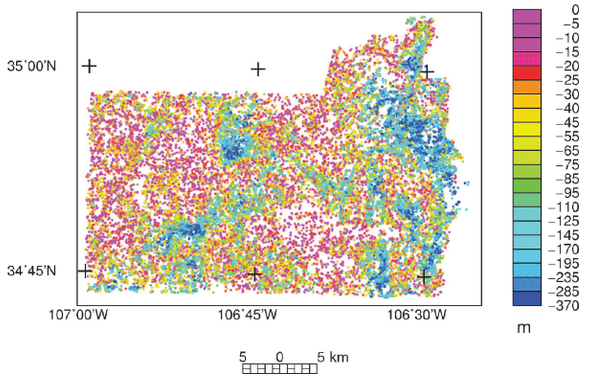

Figure 4. Werner deconvolution depth estimates for the Isleta-Kirtland area, in meters below surface.

Holstein's observation leaves open the problem of finding a suitable model for the analysis of the physical property contrast part of the solution. Unless some framework can be found in which the vertices can be treated independently, it is unikely that these data will be useful.

In its present form, the 3D multiple-source Werner algorithm does not yield useful dip angle and susceptibility information. It would be interesting to seek a modification along the lines of Mushayandebvu et al. (2004). In the meantime, the depth estimates provided by the program appear to be useful by themselves. As a practical matter, dip angle and susceptibility estimates are usually regarded as the least reliable part of Werner deconvolution output.

CONCLUSIONS

The multiple-source Werner deconvolution algorithm of Hansen and Simmonds can be generalized to three dimensions, contrary to previous conjecture, and successfully implemented. Tests on synthetic and real data show that the algorithm gives useful depth estimates and locations in a variety of settings. Furthermore, the algorithm should give depth and location estimates for gravity data in appropriate geological settings. However, the problem of calculating useful dip angle and susceptibility information is currently unsolved. Generalization of the Werner deconvolution algorithm to more general source types, both in profile form and in the 3D case considered here, is in progress.

ACKNOWLEDGMENTS

The author thanks Pearson, deRidder and Johnson, Inc. for permission to publish this work, Misac Nabighian for fruitful collaboration on the previous effort which made this work possible, and Jeff Phillips for a careful reading of this manuscript which improved it substantially. The author also thanks the assistant and associate editors and the reviewers for thoughtful suggestions, some of which opened new lines of research.

APPENDIX A

THE TWO-SOURCE CASE

Because the general case of m sources is not very intuitive, it is instructive to begin with the two-source case, where the relevant equations can be constructed explicitly. For the case of two sources at locations R_{1i} and R_{2i} the 3D extended Euler equations are

$$\left(R_{i_1} - R_{1i_1}\right)\nabla_{i_1}\mathcal{H}_j M_1 = \alpha_{1j}, \tag{A-1}$$

$$\left(R_{i_2} - R_{2i_2}\right)\nabla_{i_2}\mathcal{H}_j M_2 = \alpha_{2j}. \tag{A-2}$$

Equation 1 states that if M is a potential field satisfying a Euler equation of index 0, then so is $\mathcal{H}_j M$. Applying this result to the components of $\mathcal{H}_j M_1$ yields

$$\left(R_{i_1} - R_{1i_1}\right)\nabla_{i_1}\mathcal{H}_k\mathcal{H}_j M_1 = \alpha_{1jk}, \tag{A-3}$$

where the index k appears because each application of Nabighian and Hansen's (2001) procedure yields two additional equations. In the present notation, this results in the ap-

pearance of an extra free index. Similarly, for $\mathcal{H}_j M_2$ we have

$$\left(R_{i_2} - R_{2i_2}\right)\nabla_{i_2}\mathcal{H}_k\mathcal{H}_j M_2 = \alpha_{2jk}, \tag{A-4}$$

where α_{1jk} and α_{2jk} are constant tensors carrying the same susceptibility contrast and dip and strike angle information as α_{1j} and α_{2j}, respectively.

Because $\nabla_i\mathcal{H}_j M = \nabla_j\mathcal{H}_i M$ (proof: take the Fourier transform; in the frequency domain the result is obvious), the preceding pair of equations can be written in the form

$$\left(R_{i_1} - R_{1i_1}\right)\nabla_j\mathcal{H}_{i_1}\mathcal{H}_k M_1 = \alpha_{1jk}, \tag{A-5}$$

$$\left(R_{i_2} - R_{2i_2}\right)\nabla_j\mathcal{H}_{i_2}\mathcal{H}_k M_2 = \alpha_{2jk}. \tag{A-6}$$

A fairly obvious strategy for writing an equation which involves only the observable field $M = M_1 + M_2$ now suggests itself: contract the equation A-5 with $(R_k - R_{2k})$ and equation A-6 with $(R_k - R_{1k})$. This yields

$$\left(R_{i_1} - R_{1i_1}\right)\left(R_{i_2} - R_{2i_2}\right)\nabla_j\mathcal{H}_{i_1}\mathcal{H}_{i_2} M_1 = \left(R_{i_2} - R_{2i_2}\right)\alpha_{1ji_2}, \tag{A-7}$$

$$\left(R_{i_1} - R_{1i_1}\right)\left(R_{i_2} - R_{2i_2}\right)\nabla_j\mathcal{H}_{i_1}\mathcal{H}_{i_2} M_2 = \left(R_{i_1} - R_{1i_1}\right)\alpha_{2ji_1}, \tag{A-8}$$

where the dummy index k in the equation A-5 is changed to i_2 and in equation A-6 is changed to i_1. Adding the equations A-7 and A-8 yields the required equation involving only $M = M_1 + M_2$:

$$\begin{aligned}\left(R_{i_1} - R_{1i_1}\right)&\left(R_{i_2} - R_{2i_2}\right)\nabla_j\mathcal{H}_{i_1}\mathcal{H}_{i_2} M \\ &= \left(R_{i_2} - R_{2i_2}\right)\alpha_{1ji_2} + \left(R_{i_1} - R_{1i_1}\right)\alpha_{2ji_1}.\end{aligned} \tag{A-9}$$

Equation A-9 is to be solved for the source locations R_{1i} and R_{2i} and the constants α_{1ji_1} and α_{2ji_1} using data on the surface $z = 0$, denoted by $R_i = r_i$. To carry this out, equation A-9 is expanded in powers of r_i. Based on experience from the profile multiple-source Werner equations (Hansen and Simmonds, 1993), the terms in the alphas and those in R_{1i} and R_{2i} are kept separate:

$$\begin{aligned}&\left(R_{2i_1}\alpha_{1ji_1} + R_{1i_1}\alpha_{2ji_1}\right) - \left(\alpha_{1ji_1} + \alpha_{2ji_1}\right)r_{i_1} \\ &\quad + R_{1i_1}R_{2i_2}\nabla_j\mathcal{H}_{i_1}\mathcal{H}_{i_2} M - \left(R_{1i_1} + R_{2i_1}\right)r_{i_2}\nabla_j\mathcal{H}_{i_1}\mathcal{H}_{i_2} M \\ &= -r_{i_1}r_{i_2}\nabla_j\mathcal{H}_{i_1}\mathcal{H}_{i_2} M.\end{aligned} \tag{A-10}$$

Equation A-10 can be regarded as determining the coefficients

$$a_{0j} = \left(R_{2i_1}\alpha_{1ji_1} + R_{1i_1}\alpha_{2ji_1}\right), \tag{A-11}$$

$$a_{1ji_1} = -\left(\alpha_{1ji_1} + \alpha_{2ji_1}\right), \tag{A-12}$$

$$b_{0i_1i_2} = R_{1(i_1}R_{2i_2)} - \tfrac{1}{3}\delta_{i_1i_2}R_jR_j, \tag{A-13}$$

and

$$b_{1i_1} = -\left(R_{1i_1} + R_{2i_1}\right), \tag{A-14}$$

where $R_{1(i_1}R_{2i_2)} = 1/2(R_{1i_1}R_{2i_2} + R_{1i_2}R_{2i_1})$. The reason that the particular combination of terms occurs in equation A-13 is as follows. If A_{ij} is any tensor, it can be written uniquely as

$$A_{ij} = C_{ij} + S_{ij} + \delta_{ij}T, \tag{A-15}$$

where C_{ij} is symmetric and trace free, S_{ij} is antisymmetric, and δ_{ij} is the identity tensor. In fact, all three components can be written explicitly:

$$\begin{aligned}C_{ij} &= A_{(ij)} - \tfrac{1}{3}\delta_{ij}A_{kk} \\ &= \tfrac{1}{2}(A_{ij} + A_{ji}) - \tfrac{1}{3}\delta_{ij}A_{kk},\end{aligned} \tag{A-16}$$

$$\begin{aligned}S_{ij} &= A_{[ij]} \\ &= \tfrac{1}{2}(A_{ij} - A_{ji}),\end{aligned} \tag{A-17}$$

$$T = \tfrac{1}{3}A_{kk}. \tag{A-18}$$

If M is a potential field, then $\nabla_i\nabla_i M = 0$ by definition and $\nabla_{[i}\nabla_{j]}M = 0$ because partial derivatives commute. Contracting A_{ij} with $\nabla_i\nabla_j M$ yields

$$\begin{aligned}A_{ij}\nabla_i\nabla_j M &= C_{ij}\nabla_i\nabla_j M + S_{ij}\nabla_i\nabla_j M + \delta_{ij}T\nabla_i\nabla_j M \\ &= C_{ij}\left(\nabla_{[i}\nabla_{j]} - \tfrac{1}{3}\delta_{ij}\nabla_k\nabla_k\right)M + S_{ij}\nabla_{[i}\nabla_{j]}M \\ &\quad + T\nabla_k\nabla_k M \\ &= C_{ij}\left(\nabla_{[i}\nabla_{j]} - \tfrac{1}{3}\delta_{ij}\nabla_k\nabla_k\right)M.\end{aligned} \tag{A-19}$$

This says that everything except the trace-free, symmetric part of A_{ij} drops out; neither the antisymmetric part nor the trace is present in any equation in which this contraction appears. Here, $A_{ij} = R_{1i}R_{2j}$, so

$$R_{1i}R_{2j}\nabla_i\nabla_j M = \left(R_{1[i}R_{2j]} - \tfrac{1}{3}\delta_{ij}R_{1k}R_{2k}\right)\nabla_i\nabla_j M. \tag{A-20}$$

The coefficients $b_{0i_1i_2}$ and b_{1i_1} are identical to those that occur in the two-source case of the multiple-source Euler algorithm (Hansen and Suciu, 2002). Thus, the same procedure used there can be followed to extract the source locations. It will be shown that this situation persists in the case of m sources.

For the profile multiple-source Werner algorithm, the alphas can be extracted from the coefficients a_{0j} and a_{1ji_1} once the source locations have been determined. Rearrangement of the equations defining a_{0j} and a_{1ji_1} yields

$$\left(R_{1i_1} - R_{2i_1}\right)\alpha_{1ji_1} = -\left(a_{0j} + a_{1ji_1}R_{1i_1}\right), \tag{A-21}$$

$$\left(R_{2i_1} - R_{1i_1}\right)\alpha_{2ji_1} = -\left(a_{0j} + a_{1ji_1}R_{2i_1}\right). \tag{A-22}$$

The alphas are generally underdetermined because there are only three equations, whereas usually the alphas have five independent components each. However, if the sources are contacts, only three of these components are independent and the dip angle, susceptibility, and strike direction can be determined, as described in the text.

REFERENCES

Dongarra, J. J., C. B. Moler, J. R. Bunch, and G. W. Stewart, 1979, LINPACK Users' Guide: Society of Industrial and Applied Mathematics.

Grauch, V. J. S., 2001, Using high-resolution aeromagnetic surveys to map subsurface hydrogeology in sediment-filled basins: A case study over the Rio Grande rift, central New Mexico, USA: Exploration Geophysics, **32**, 209–213.

Hansen, R. O., and M. Simmonds, 1993, Multiple-source Werner deconvolution: Geophysics, **58**, 1792–1800.

Hansen, R. O., and L. Suciu, 2002, Multiple-source Euler deconvolution: Geophysics, **67**, 525–535.
Hansen, R. O., and X. Wang, 1988, Simplified frequency-domain expressions for potential fields of arbitrary three-dimensional bodies: Geophysics, **53**, 365–374.
Hartman, R. R., D. J. Teskey, and J. L. Friedberg, 1971, A system for rapid aeromagnetic interpretation: Geophysics, **36**, 891–918.
Li, X., 2003, On the use of different methods for estimating magnetic depth: The Leading Edge, **22**, 1090–1099.
Mushayandebvu, M. F., V. Lesur, A. B. Reid, and J. D. Fairhead, 2004, Grid Euler deconvolution with constraints for 2D structures: Geophysics, **69**, 489–496.
Mushayandebvu, M. F., P. van Driel, A. B. Reid, and J. D. Fairhead, 2001, Magnetic source parameters of two-dimensional structures using extended Euler deconvolution: Geophysics, **66**, 814–823.
Nabighian, M. N., 1972, The analytic signal of two-dimensional bodies with polygonal cross-section: Its properties and use for automated interpretation: Geophysics, **37**, 507–517.
———, 1984, Toward a three-dimensional automatic interpretation of potential field data via generalized Hilbert transforms: Fundamental relations: Geophysics, **49**, 780–786.
Nabighian, M. N., and R. O. Hansen, 2001, Unification of Euler and Werner deconvolution in three dimensions via the generalized Hilbert transform: Geophysics, **66**, 1805–1810.
Ostrowski, J. S., M. Pilkington, and D. J. Teskey, 1993, Werner deconvolution for variable altitude aeromagnetic data: Geophysics, **58**, 1481–1490.
Phillips, J. D., 2002, Two-step processing for 3D magnetic source locations and structural indices using extended Euler or analytic signal methods: 72nd Annual International Meeting, SEG, Expanded Abstracts, 727–730.
Reid, A. B., J. M. Allsop, H. Granser, A. J. Millett, and I. W. Somerton, 1990, Magnetic interpretation in three dimensions using Euler deconvolution: Geophysics, **55**, 80–91.
Thurston, J. B., and R. S. Smith, 1997, Automatic conversion of magnetic data to depth, dip, and susceptibility contrast using the SPI™ method: Geophysics, **62**, 807–813.
U.S. Geological Survey and Sander Geophysics Ltd., 1998, Digital data from the Isleta-Kirtland aeromagnetic survey, collected south of Albuquerque, New Mexico: U.S. Geological Survey Open-File Report 98-341.